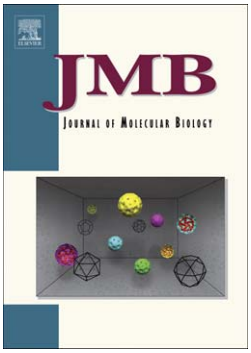

Dissecting CNBP, a zinc-finger protein required for neural crest development, in its structural and functional domains

Pablo Armas, Tristán H. Agüero, Mariana Borgognone, Manuel J. Aybar, Nora B. Calcaterra

PII: S0022-2836(08)00948-0
DOI: doi: 10.1016/j.jmb.2008.07.079
Reference: YJMBI 60688

To appear in: *Journal of Molecular Biology*

Received date: 25 April 2008
Revised date: 25 July 2008
Accepted date: 28 July 2008

Please cite this article as: Armas, P., Agüero, T.H., Borgognone, M., Aybar, M.J. & Calcaterra, N.B., Dissecting CNBP, a zinc-finger protein required for neural crest development, in its structural and functional domains, *Journal of Molecular Biology* (2008), doi: 10.1016/j.jmb.2008.07.079

Running title: CNBP structural and functional domains

DISSECTING CNBP, A ZINC-FINGER PROTEIN REQUIRED FOR NEURAL CREST DEVELOPMENT, IN ITS STRUCTURAL AND FUNCTIONAL DOMAINS

Pablo Armas[1], Tristán H. Agüero[2], Mariana Borgognone[1], Manuel J. Aybar[2], and Nora B. Calcaterra[1]*

[1] División Biología del Desarrollo, IBR (Instituto de Biología Molecular y Celular de Rosario), Consejo Nacional de Investigaciones Científicas y Técnicas (CONICET) - Área Biología General, Dpto. de Ciencias Biológicas, Facultad de Ciencias Bioquímicas y Farmacéuticas, Universidad Nacional de Rosario. Suipacha 531, (S2002LRK) Rosario, Argentina.

[2] Dpto. Biología del Desarrollo, INSIBIO (CONICET-Universidad Nacional de Tucumán), Chacabuco 461, T4000ILI – San Miguel de Tucumán, Tucumán, Argentina.

*Corresponding author: Nora B. Calcaterra, IBR – CONICET, Área Biología General, Dpto. de Ciencias Biológicas, Facultad de Ciencias Bioquímicas y Farmacéuticas, Universidad Nacional de Rosario, Suipacha 531, (S2002LRK) Rosario, Argentina; Tel./Fax: 54 – 341 – 4804601; *E*-mail: calcaterra@ibr.gov.ar

ABSTRACT

Cellular Nucleic Acid Binding Protein (CNBP) plays an essential role in forebrain and craniofacial development by controlling cell proliferation and survival to mediate neural crest expansion. CNBP binds to single-stranded nucleic acid and displays nucleic acid chaperone activity *in vitro*. CNBP family shows a conserved modular organization of seven Zn knuckles and an RGG box between the first and second Zn knuckles. The participation of these structural motifs in CNBP biochemical activities has still not been addressed. Here, we describe the generation of CNBP mutants that dissect the protein into regions with structurally and functionally distinct properties. Mutagenesis approaches were followed to generate: i) an amino acid replacement that disrupted the fifth Zn-knuckle, ii) N-terminal deletions that removed the first Zn knuckle and the RGG box or the RGG box alone, and iii) a C-terminal deletion that eliminated the three last Zn-knuckles. Mutant proteins were overexpressed in *Escherichia coli*, purified, and used to analyze their biochemical features *in vitro* or overexpressed in *Xenopus laevis* embryos to study their function *in vivo* during neural crest cell development. We found that the Zn knuckles are required but not individually essential for CNBP biochemical activities whereas the RGG box is essential for RNA-protein binding and nucleic acid chaperone activity. The RGG box removal allowed CNBP to preserve a weak ssDNA binding capability. A mutant mimicking the natural N-terminal proteolytic CNBP form behaved as the RGG deleted mutant. By gain- and loss-of-function experiments in *Xenopus* embryos we confirmed the participation of CNBP in neural crest development, and we demonstrated that the CNBP mutants lacking the N-terminal region or the RGG box alone may act as dominant negatives *in vivo*. Based on these data, we speculate about the existence of a specific proteolytic mechanism for the regulation of CNBP biochemical activities during neural crest development.

Key words: Cellular nucleic acid binding protein, Zn knuckle, RGG box, nucleic acid chaperone, single-stranded nucleic acid binding, neural crest development.

INTRODUCTION

Craniofacial malformations are involved in three fourths of all congenital birth defects in humans, affecting the development of head, face, or neck [1]. Although tremendous progresses in the study of craniofacial development have been made, the molecular and cellular mechanisms underlying how rostral head structure formation takes place are still largely unknown. One of the key features of craniofacial development is the formation of cranial neural crest cells. The specification, emigration and migration, proliferation, survival, and ultimate fate determination of these cells play an important role in regulating craniofacial development. Several proteins have been reported to be required for cranial neural crest cells fate, proliferation, and survival control. Cellular Nucleic Acid Binding Protein (CNBP) is one of those proteins showing specific anterior expression patterns in chick, zebrafish, mouse and *Xenopus* embryos [2-5].

CNBP is a single-stranded nucleic acid binding protein able to bind to single-stranded DNA (ssDNA) and RNA molecules. CNBP binding to ssDNA was reported to be involved in both negative [6-8] and positive [9,10] transcriptional regulation. Interacting with RNA, CNBP was reported as a transcriptional[11] as well as a translational [12,13] modulator. Likely, CNBP may perform this broad spectrum of actions by means of its nucleic acid chaperone activity. Nucleic acid chaperones are nucleic acid binding proteins that catalyze the rearrangement of nucleic acids into conformations containing the maximum number of complementary base pairs. These proteins randomly disrupt the misformed bonds via ATP-independent repeated cycles of binding and release and, thus, facilitate the folding of the thermodynamically most stable three-dimensional structure needed for nucleic acid biological function [14-17]. The nucleic acid chaperone activity may allow CNBP to control transcriptional processes through chromatin structure remodeling of promoter regions and/or translational processes by affecting RNA structures that finally modulate the action of specific trans-acting factors [18].

Amino acid sequence analysis of the CNBP family reveals the presence of two remarkable structural features (Figure 1). Firstly, CNBP is mainly formed by seven CCHC zinc knuckle motifs that exhibit striking sequence similarities with the corresponding structure of retroviral nucleocapsid (NC) proteins [6]. These zinc knuckles have amino acids arrangements with the consensus sequence "C–ϕ–X–C–G–±–X–G–H–X_3–δ–C ", where X = variable amino acid, ϕ = aromatic amino acid, ± = charged amino acid, and δ = carbonyl-containing residue. As anticipated from this structural conservation, most of the CCHC zinc knuckles from human CNBP are capable of replacing HIV-1 NC protein zinc knuckles without affecting viral structure and function [19]. Secondly, CNBP contains a peculiar arginine/glycine-rich region between the first and second Zn knuckles, which is highly similar to the RGG box proposed as an RNA binding motif and as a predictor of RNA binding activity [20]. Additionally, CNBP presents natural shorter forms. The primary structure shows a PEST putative proteolytic site likely responsible for a shorter protein form that lacks the first Zn knuckle and the RGG box motifs [21-23]. Moreover, the CNBP primary transcript may suffer the alternative splicing of its second intron to render a complete polypeptide (α-CNBP form) or a shorter one (β-CNBP form) [8,24-26]. Depending on the species, β-CNBP forms lack a region of 6 to 16 amino acids located between the RGG box and the second Zn knuckle.

A central question that at this point is worth addressing is which structural motif(s) are required for CNBP biological function. We aimed our studies first to identify which motif(s) are involved in *in vitro* protein-nucleic acid binding and nucleic acid chaperone activities, then to confirm these requirements *in vivo* during neural crest development. Several mutant versions of *Chaunus arenarum* (formerly named *Bufo arenarum*) CNBP were produced by amino acid or deletion site-directed mutagenesis to map the contribution of different motifs to the CNBP biochemical activities. The amino acid changed and the domains deleted were selected according to the recognition of conserved residues or structural modules. The

different mutant proteins were expressed as recombinant proteins, purified and tested in gel retardation assays for their nucleic acid binding properties and in nucleic acid annealing and melting assays for their nucleic acid chaperone activity features. We found that the RGG box and the Zn knuckles are needed for maximal CNBP biochemical activities. The RGG box is involved in differential target–binding specificity and it is required for nucleic acid binding and chaperone activities. Conversely, the Zn knuckles contribute to reach the maximal biochemical activities. Interestingly, we found that a CNBP mutant mimicking the natural proteolytic form displayed the most differential biochemical behavior. The removal of the N-terminal region yielded a protein unable to bind to RNA or to act as nucleic acid chaperone even though it conserved a weak ssDNA binding capability. The requirement of the N-terminal region for CNBP function during the early steps of neural crest development was confirmed *in vivo* by microinjecting *Xenopus laevis* embryos with mRNAs coding for the wild type and different CNBP mutant forms and subsequent analyses of neural crest marker genes expression patterns.

RESULTS

The CNBP structure-function relationship was analyzed in order to identify the major structural and functional protein domains responsible for single-stranded nucleic acid binding and chaperone activities. The role of individual or grouped motifs in CNBP functionality was evaluated by generation of amino acid or deletion site-directed mutations. The strategy was to functionally disrupt or remove the motifs of interest leaving the rest of the protein intact and, then, to analyze RNA and ssDNA binding and oligonucleotide annealing and melting promotion activities. Those CNBP mutants that showed the most noticeable differences compared to the wild type α-CNBP form ($CNBP_{WT}$) were subsequently analyzed *in vivo* during the early steps of *Xenopus* neural crest development.

Generation of amino acid site-directed CNBP mutants

Among the seven CCHC zinc knuckles present in CNBP, the fifth is the only one unable to structurally and functionally substitute the first CCHC zinc knuckle present in the HIV-1 NC protein [19]. This domain was suggested as non-functional in nucleic acid binding and addressed to other functions [19], thus arising as an interesting target for structural-functional studies. The zinc knuckles from retroviral NC proteins contain an absolutely conserved histidine that is essential for protein functions [15]. Therefore, we studied the requirement of the fifth CNBP Zn-knuckle by replacing the histidine 128 of *Chaunus arenarum* CNBP by alanine ($CNBP_{H128A}$) and, as the net charge of the NC protein zinc knuckle is important for its functionality [19], by glutamine ($CNBP_{H128Q}$), or aspartic acid ($CNBP_{H128D}$) (Figure 2). Substitution by alanine was expected to disrupt the zinc-binding site in the motif by eliminating one of the four metal coordination ligands without affecting the knuckle

conformation. In contrast, substitutions by aspartic acid or glutamine were supposed to cause greater conformational changes than the one caused by alanine in addition to the disruption of the metal binding site.

Generation of deletion site-directed CNBP mutants

CNBP shows a highly conserved modular structural organization consisting of an RGG box and seven CCHC zinc knuckles motifs (Figure 1). There exists functional and structural equivalence among most of the CNBP CCHC motifs and the retroviral zinc knuckles from the HIV-1 NC protein [19]. It was proposed that the CCHC zinc knuckles are responsible for the NC nucleic acid binding and chaperone activities [15]. The RGG box motif has also been largely involved in nucleic acid binding [27-30] and in nucleic acid chaperone activities [31-33]. Therefore, it is difficult to accurately assign *a priori* the role of each of these motifs in the CNBP mechanism of action.

To survey the role of each CNBP motif type, we generated CNBP mutants that precisely deleted the major predicted domains (Figure 2). One of the CNBP deletion mutants, $CNBP_{\Delta RGG}$, was generated by removing the whole RGG motif (amino acids 22 to 37). Another CNBP deletion mutant, $CNBP_{\Delta 1\text{-}RGG}$, was generated by deletion of the first zinc knuckle together with the RGG box (amino acids 1 to 50). It is worth mentioning that the $CNBP_{\Delta 1\text{-}RGG}$ mutant was designed to obtain a protein identical to the shorter CNBP form previously reported for *X. laevis* and *C. arenarum* as a natural proteolytic product [21,23]. Finally, a C-terminal deletion mutant, $CNBP_{\Delta 5\text{-}7}$, was generated by removing the three last CCHC motifs (amino acids 127 to 178), but leaving unchanged the first four zinc knuckles and the RGG box.

ssDNA and RNA-binding assays show differential binding requirements dependent on the nucleic acid nature

The CNBP mutant forms were evaluated by electrophoretic mobility shift assays (EMSA) using previously reported ssDNA or RNA CNBP targets [18,24].

No differential EMSA pattern was observed between $CNBP_{WT}$ and amino acid site-directed mutants when the RNA-L4-UTR probe was used (Figure 3a). Conversely, the same CNBP mutants displayed apparent lower affinities for the Comp-CT ssDNA probe (Figures 3b and S1a in Supplementary Material). A similar behavior was observed with $CNBP_{\Delta 5\text{-}7}$ (Figures 4a, 4b, and S1b in Supplementary Material).

A more drastic effect of the mutations was observed when $CNBP_{\Delta 1\text{-}RGG}$ and $CNBP_{\Delta RGG}$ were analyzed. Both mutants failed to bind to the RNA probe, even at 100 μM of each deletion mutant (Figure 4a). In addition to this, $CNBP_{\Delta 1\text{-}RGG}$ and $CNBP_{\Delta RGG}$ bound to Comp-CT ssDNA with affinities significantly lower even than those showed by amino acid and $CNBP_{\Delta 5\text{-}7}$ site-directed mutants (Figures 4b and S1b in Supplementary Material). Moreover, $CNBP_{\Delta 1\text{-}RGG}$ bound to Comp-CT ssDNA with significantly lower affinity than $CNBP_{\Delta RGG}$ (Figures 4b and S1b in Supplementary Material). The discrepant behavior observed between RNA and ssDNA probes may be due to differences in the primary sequence and/or to the nature of the probes. Hence, we analyzed by EMSA the CNBP mutants binding to a ssDNA probe that represents the 5'UTR sequence from *X. laevis* L4 rp-mRNA (DNA-L4-UTR)[18,24]. No differences in the DNA-L4-UTR binding were observed among all the mutants and $CNBP_{WT}$ (Figures 3c and 4c). This finding suggests that N-terminal deletion mutants possess a differential target binding specificity, which depends on the nucleic acid nature (i.e. RNA or ssDNA).

The RGG box is the major motif responsible for nucleic acid chaperone activity

The nucleic acid chaperone activity of each of the CNBP mutants generated in this work was evaluated through complementary oligonucleotide annealing and melting promotion assays according to previous reports [18,34].

Amino acid site-directed mutants showed annealing rates faster than controls, but lower than $CNBP_{WT}$ (Figure 5a and 5c). A similar behavior was observed for the $CNBP_{\Delta 5\text{-}7}$ mutant (Figure 5a and 5c). The most important differences were detected when $CNBP_{\Delta 1\text{-}RGG}$ and $CNBP_{\Delta RGG}$ were evaluated. Both mutants failed to promote the annealing of complementary oligonucleotides. Moreover, in their presence annealing rates were significantly lower than in the presence of $CNBP_{WT}$ and even lower than in control reactions (Figure 5b and 5c). $CNBP_{\Delta RGG}$ and $CNBP_{\Delta 1\text{-}RGG}$ were unable to promote nucleic acid annealing whereas they preserve, at least partially, the capacity of binding to ssDNA. Therefore, the decrease in the duplex formed might be due to the conjunction of both the inability of the protein to promote the annealing and its ability to weakly bind and sequester the ssDNA Comp-CT strand.

In regard to the melting promotion activity, amino-acid (not shown) as well as $CNBP_{\Delta 5\text{-}7}$ mutants displayed a similar behavior to the $CNBP_{WT}$, i.e. they lowered the duplex melting temperature to ≈ 35ºC. On the other hand, $CNBP_{\Delta 1\text{-}RGG}$ and $CNBP_{\Delta RGG}$ were not able to lower oligonucleotide melting temperature, which remained over 60ºC (Figure 6a). These results may be due to an increment of CNBP mutants' thermal denaturation susceptibility or to a specific loss of CNBP mutants melting activity. To address this, we performed EMSAs using $CNBP_{WT}$ and deletion mutant proteins that were maintained at 4ºC or thermally stressed following the same heating program used in melting assays. Thermal stress slightly reduced the nucleic acid binding capability of mutants, but the same reduction was observed for the wild type form (Figure 6b). This finding indicates that the N-terminal deletions did not cause

an increment in thermal denaturation susceptibility, and that the N-terminal region is actually required for melting promotion activity.

Taken together, the results suggest that Zn-knuckles of the C-terminal region contribute to reach the CNBP maximal nucleic acid chaperone activity, however, the actual structural requirement for CNBP annealing and melting promotion activities is the N-terminal region. In view of $CNBP_{\Delta 1\text{-}RGG}$ and $CNBP_{\Delta RGG}$ mutants do not contain the RGG box it is tempting to speculate that the RGG box is the main structural domain required for the CNBP nucleic acid chaperone activity.

The N-terminal region is essential for CNBP function *in vivo*

CNBP is highly expressed in head forming regions of different vertebrate embryos [2-5]. Recently, it was demonstrated that CNBP knockdown produced a decrease in the expression of neural crest marker genes in zebrafish embryos (i.e., *foxD3*, *ap2*α, and *crestin*)[5]. We decided to explore *in vivo* the CNBP structural requirements considering its putative function in *Xenopus laevis* neural crest development. We chose *X. laevis* according to three major reasons. First, *X. laevis* and *C. arenarum* CNBPs are 99.9% identical [22]. Second, neural crest gene markers expression patterns are well known in *X. laevis* [35]. Third, this model organism is one of the most favorable experimental models for genetic overexpression. Indeed, *X. laevis* embryos are easily injected with mRNA, and the first cleavage during segmentation divides the embryo into two identical cells. Therefore, one half of the embryo can be used as the experimental side and the other as the control.

In this work, we analyzed by whole-mount *in situ* hybridization the expression of two key genes of neural crest specification cascade, *foxD3* and *c-myc,* in embryos microinjected with mRNAs coding for $CNBP_{WT}$, $CNBP_{\Delta 5\text{-}7}$, $CNBP_{\Delta 1\text{-}RGG}$, and $CNBP_{\Delta RGG}$. *FoxD3* is one of the

earliest neural crest genes to be expressed in mice, zebrafish, *Xenopus*, and chick embryos, and one of the most reliable specification markers [36,37]. The protooncogene *c-myc* is expressed early in the neural plate border (the prospective neural crest), and it is an essential early regulator of neural crest formation in *Xenopus* embryos [38]. Moreover, *c-myc* is one of the reported CNBP targets [3,9].

Xenopus laevis embryos were microinjected with the different mRNAs, and subsequently the expression of neural crest territory markers was evaluated by whole mount *in situ* hybridization (Figure 7a-j). The marker genes expression levels were estimated by measuring their expression areas in the surface of the embryo. This methodology may underestimate the magnitude of the effect produced by the injection of embryos. Actually, this procedure reveals the gene expression in cells of the most superficial layers of the embryo but not in those deeper ones. It is worth mentioning that the observed effect was always of the same type and followed the same pattern for all microinjected RNA amounts. The main difference was the amount of affected embryos in relation with the amount of mRNA microinjected; i.e., when higher amounts of mRNA were injected, higher percentages of affected embryos were observed. For most of the experiments, 3 ng of mRNA were microinjected per embryo since it was the lowest amount of mRNA that caused the maximal and reproducible effect. Embryos were observed and analyzed as indicated in Experimental Procedures. First, we measured the expression areas of each gene marker in control and microinjected embryo sides. Embryos that showed gene expression areas different in at least 30 % in the injected side compared with the control side were classified as affected. Then, the expression areas of the affected embryos were averaged and the observed differences were expressed as percentages of increase or decrease compared with the not injected control side.

The injection of the $CNBP_{WT}$ mRNA leaded to an expansion of the neural crest territory analyzed by the expression of *foxD3* and *c-myc*. From 55 injected embryos, 54% showed an

increase of 61 ± 12 % in the *foxD3* territory in the injected side compared with the not injected control side (Figure 7a) and 54% of the injected embryos (n=48) showed an 85 ± 19 % increase in the *c-myc* territory (Figure 7b). These data confirm the participation of CNBP in the early events of *Xenopus* neural crest induction.

Next we analyzed the *in vivo* functionality of $CNBP_{\Delta RGG}$ and $CNBP_{\Delta 1\text{-}RGG}$ by overexpressing each mutant in *Xenopus* embryos. The injection of $CNBP_{\Delta RGG}$ mRNA (Figure 7c and d) produced a decrease in the expression level of *foxD3* and *c-myc.* Indeed, 56% of the injected embryos (n=54) showed a 35 ± 5 % reduction of the *foxD3* expression area, and 53% of the injected embryos (n=57) showed a 48 ± 5 % reduction of the *c-myc* expression territory. Regarding the $CNBP_{\Delta 1\text{-}RGG}$ mutant, 50% of the injected embryos (n=32) showed a 45 ± 6 % reduction of *foxD3* expression area (Figure 7e) and 42% of the injected embryos showed a 72 ± 5 % reduction of *c-myc* expression area (Figure7f). The injection of $CNBP_{\Delta 5\text{-}7}$ mRNA produced only a slight effect on the expression of *c-myc* gene while *foxD3* marker remained almost unchanged (not shown). To address whether the injected mRNAs were efficiently translated, we compared the CNBP levels in treated and not treated embryos by Western blot. These assays showed that microinjected embryos expressed similar CNBP levels, which were at least 5-fold higher than the detected one in not injected embryos (Figure S2).

The embryonic development is a highly regulated process and the effect described above might be due to multiple reasons. Therefore, it was essential to address whether the marker genes expression differences observed were a specific consequence of the mutants overexpression or a pleiotropic unspecific effect caused by the embryo manipulation. For this purpose, we performed the following rescue experiments. Embryos were co-injected with the same amount of mRNA that codes for each CNBP deletion mutant and $CNBP_{WT}$, then the expression of the neural crest marker genes was analyzed. Embryos overexpressing

$CNBP_{\Delta RGG}$ and $CNBP_{WT}$ showed rescued expression of *c-myc* (86% of the injected embryos with normal expression in the injected side, n=35, Figure 7h) and *foxD3* (71%, n=41, Figure 7g). When the mRNA of $CNBP_{\Delta 1\text{-}RGG}$ and $CNBP_{WT}$ were co-injected a rescue in the expression of *c-myc* (79%, n=57, Figure 7j) and *foxD3* (73%, n=59, Figure 7i) was also observed.

These results show that CNBP is required for the expression of neural crest genes during *Xenopus laevis* early specification process, and that its activity can be specifically blocked by different types of mutants with dominant negative effects. Moreover, these experiments confirm that the N-terminal region, likely the RGG box, is an important CNBP functional domain not only *in vitro* but also *in vivo*.

DISCUSSION

Here we have presented data that characterize the biochemical and functional properties of CNBP. In this study, we have taken advantage of the commonly used approach of producing rational mutations in order to analyze the relevance of individual or grouped motifs in protein biochemical and biological functions. Several amino acid replacement and deletion site-directed mutants of the *Chaunus arenarum* CNBP were produced, purified, and tested for nucleic acid binding and nucleic acid chaperone (melting an annealing) activities. The design of the mutant constructs was made according to a detailed inspection of the protein sequence and functional domains and the identification of a conserved modular arrangement among all CNBP family members. Results obtained *in vitro* were validated *in vivo* by means of gain- and loss-of-function experiments in *Xenopus laevis* embryos.

Functional mutant analysis defines that the N-terminal region is essential for CNBP biochemical activities

Amino acid site-directed and $CNBP_{\Delta 5\text{-}7}$ mutants did not show differential EMSA patterns with the RNA probe. The same mutants bound to Comp-CT ssDNA with apparent lower affinity than $CNBP_{WT}$, but bound to the DNA-L4-UTR probe with no differences. It was demonstrated that CNBP affinity by its targets depends on the nature of the nucleic acids (RNA or ssDNA) and also on the extension of G-rich single-stranded stretches present inside their secondary structures [18]. Comp-CT secondary structure contains more unpaired-G residues than DNA-L4-UTR or RNA-L4-UTR and, consequently, these nucleic acids are bound by CNBP with different affinities. Indeed, the K_d for Comp-CT is about 100-fold lower than those for DNA-L4-UTR or RNA-L4-UTR [18]. Most likely, the high binding

affinity of CNBP to Comp-CT allowed us to detect slight differences in binding behavior between $CNBP_{WT}$ and amino acid and $CNBP_{\Delta 5\text{-}7}$ site-directed mutants. Substitution of the conserved histidine by alanine in retroviral NC protein zinc knuckles did not affect their capability of zinc binding [39], but caused a drop in RNA binding [40]. Perhaps, a similar effect took place in the case of CNBP when the histidine from the fifth Zn knuckle was substituted or the three C-terminal Zn knuckles were removed, but the remaining Zn knuckles, together with the RGG box, compensated and/or hid the loss of function. On the other hand, results from EMSAs with the Comp-CT ssDNA probe suggest that the number of functional Zn knuckles is important to reach the maximal binding capacity.

Amino-acid site directed mutants showed nucleic acid chaperone activity slightly lower than the wild type protein while similar to the $CNBP_{\Delta 5\text{-}7}$ mutant. Proteins displaying nucleic acid chaperone activity bind to unfolded or misfolded nucleic acids and facilitate their rearrangement into more stable conformations [14,15,17]. Thus, the slightly lower nucleic acid chaperone activities displayed by all these mutants might be due to a decrease in their binding capabilities that, consequently, impairs their annealing or melting promotion activities. A similar correlation between nucleic acid binding and chaperone activities has been reported in a mutational analysis of FMRP [31]. Therefore, our results suggest that zinc knuckles are partially contributing to the nucleic acid binding affinity and, consequently, to the nucleic acid chaperone activity. The common characteristic among these mutants is the absence of a functional fifth Zn knuckle. Thus, the requirement of this structural motif for optimal CNBP activities should not be completely ruled out.

The two CNBP mutations affecting the N-terminal region ($CNBP_{\Delta RGG}$ and $CNBP_{\Delta 1\text{-}RGG}$) yielded proteins that failed to bind to RNA and bound to Comp-CT ss-DNA with lower affinities even lower than the other mutants generated in this work. The lowest affinity was shown by $CNBP_{\Delta 1\text{-}RGG}$. The major difference between $CNBP_{\Delta RGG}$ and $CNBP_{\Delta 1\text{-}RGG}$ is the

absence of the first Zn knuckle. This fact reinforces our proposal that Zn knuckles partially contribute to improve the ssDNA binding capability. Moreover, both mutants were unable to display annealing and melting promoting activities. The common feature of $CNBP_{\Delta RGG}$ and $CNBP_{\Delta 1\text{-}RGG}$ is the absence of the RGG box. This finding suggests that the RGG box is not only required for optimal ssDNA binding but also essential for RNA-binding and nucleic acid chaperone activities. The requirement of the RGG box for the RNA binding and nucleic acid chaperone activity was also reported for other proteins, e.g., FMRP [31], hnRNP A1 [33], and nucleolin [32]. Taken together, the results from mutants generated in this work allow us to propose that individual Zn knuckles partially contribute to the single-stranded nucleic acid binding while the N-terminal region, likely the RGG box, is involved in nucleic acid type specificity and is essential for RNA binding and nucleic acid chaperone activities.

The HIV-1 NC nucleic acid chaperone activity is based on two related activities, hybridization and helix-destabilization [15]. Hybridization activity is sequence-unspecific and depends on the positive charges of basic amino acids. The positive charges act as counter ions of the nucleic acid phosphate backbone and facilitate annealing of complementary strands through avoiding electrostatic repulsion. Helix-destabilization activity is relatively weak and depends on the zinc knuckles because of their preference for binding single-stranded (unpaired) nucleotides. Based on the important contribution of the RGG box to the CNBP nucleic acid chaperone activity, we propose that this motif may act as a potent basic core probably functioning in a sequence-unspecific way and remodeling the nucleic acids secondary structure in order to yield a better binding target. On the other hand, the CNBP zinc knuckles may contribute in a sequence-specific fashion to the nucleic acid chaperone activity by binding to and stabilizing single-stranded unpaired nucleobases.

The N-terminal region is essential for CNBP biological function during neural crest development

Once identified the major structural motifs required for CNBP biochemical activities *in vitro* we wondered if they were also required for the CNBP biological function *in vivo*. CNBP plays an essential role in vertebrate embryonic development since depleted mouse, chicken, and zebrafish embryos show forebrain development truncation and severe craniofacial malformations [2,3,5]. Recently, we showed that the predominant function for CNBP during forebrain development is to control the balance between neural crest cell proliferation and cell survival during craniofacial development [5]. In this work, we took advantages of the *X. laevis* animal model to further analyze the CNBP biological role during vertebrate embryonic development and the *in vivo* biochemical requirements of CNBP structural regions. Our data from *in vivo* overexpression in *Xenopus* embryos allowed us to arrive at three main conclusions. First, CNBP acts upon the cascade responsible for the neural crest development in *X. laevis. C-myc* and *foxD3* expression areas showed a direct and specific relationship with the level of wild type or CNBP mutants. It is tempting to speculate that CNBP is directly involved in the molecular mechanisms controlling these essential regulators genes, but such possibility should be carefully analyzed. Second, $CNBP_{\Delta RGG}$ and $CNBP_{\Delta 1\text{-}RGG}$ act as dominant negative proteins *in vivo.* $CNBP_{WT}$ overexpression expanded the *c-myc* and *foxD3* expression areas while overexpression of $CNBP_{\Delta RGG}$ and $CNBP_{\Delta 1\text{-}RGG}$ caused a reduction in the expression areas of both neural crest gene markers. Third, the integrity of the N-terminal region, possibly the presence of the RGG box, is a requirement for *in vivo* CNBP function.

Regarding the natural short CNBP forms, β-CNBP, generated by alternative splicing, does not lose the RGG box but instead has a shorter relative distance between the RGG box motif and the second Zn knuckle. This change may affect the architecture and spatial motifs

arrangement but *a priori* the consequences in nucleic acid binding and chaperone activities would not be critical. On the other hand, the loss of the N-terminal motifs in the natural proteolytic CNBP form may have more relevant consequences in nucleic acid binding and chaperone activities. This proteolytic CNBP form is mimicked by the $CNBP_{\Delta 1\text{-}RGG}$ mutant, which failed to bind RNA and did not show nucleic acid chaperone activity and, furthermore, acted as dominant negative *in vivo.* This finding rekindles the interest of assigning a putative biological role to the proteolytic CNBP form and allows us to speculate that a specific proteolysis may exist as a cellular strategy for a CNBP biochemical activity regulation. However, further experimental evidence is needed to probe this hypothesis.

EXPERIMENTAL PROCEDURES

Mutant and wild type CNBP recombinant proteins

The cDNA sequence coding for the α form of *Chaunus arenarum* CNBP (*b*CNBP), GenBank Accession Number **AF144698** [22], was fused to an N-terminal glutathione-S-transferase (GST) tag in pGEX-2T plasmid vector (Amersham Biosciences – GE Helthcare). Site-directed deletion CNBP mutants $CNBP_{\Delta RGG}$, $CNBP_{\Delta 1\text{-}RGG}$, and $CNBP_{\Delta 5\text{-}7}$ (Figure 2) were generated from the wild type cDNA by PCR or enzyme restriction. Site-directed amino acid CNBP mutants $CNBP_{H128A}$: $CNBP_{H128D}$, and $CNBP_{H128Q}$ (Figure 2) were generated by the "megaprimer" method [41]. cDNAs used for *in vivo* experiments were cloned into pCS2+ plasmid. GST fusions were expressed in *Escherichia coli* DH5α and purified to homogeneity by affinity chromatography using Gluthathione Sepharose (Amersham Biosciences – GE Helthcare) according to the manufacturer's instructions. Purification quality was determined by SDS-PAGE and silver staining. Fusion proteins molar concentration was accurately estimated by densitometric analysis of SDS-PAGE Coomassie Brilliant Blue stained gels. The correct folding of GST fusion proteins was determined by the general secondary structure content through 200-300 nm circular dichroism spectra in a Jasco-810 spectropolarimeter.

Electrophoretic mobility shift assay (EMSA)

EMSAs were performed as described elsewhere [18]. Briefly, binding reactions were performed in 20 µl final reaction volume for 30 min at 37 ºC (20 mM HEPES, pH 8.0, 100 mM NaCl, 10 mM $MgCl_2$, 1 mM EDTA, 1 mM DTT, 1 µg/µl BSA and 10% glycerol). For ssDNA probes, 0.01 µg/µl of poly(dI:dC)·(dC:dI) and 0.5 µg/µl Heparin were added as non-specific competitors. For RNA probes, 1 µg/µl of Type VI Torula Yeast RNA as non-specific

competitor and 0.5 U/µl RNasin (Promega) were added. [^{32}P]-labeled probes were added to a final concentration of 2 nM and purified fusion proteins were added at different concentrations as indicated. Reactions were run into polyacrylamide gels containing 5% glycerol in TBE 0.5X, and gels were dried and exposed to X-Ray films for autoradiography, or Storage Phosphor Screen (Amersham Biosciences – GE Helthcare) that was subsequently scanned in a STORM 860 PhosphorImager using ImageQuant 5.2 software. Apparent dissociation constants (K_d) were estimated from the intensity of radioactive bands in EMSAs as previously described [18]. ssDNA EMSAs were performed using a probe representing the purine-rich strand of the CT element from the human *c-myc* promoter (Comp-CT), or a probe representing the 5' UTR from *X. laevis* L4 rp-mRNA (DNA-L4-UTR) [18]. RNA EMSAs were performed using a probe synthesized by *in vitro* transcription of the 5' UTR from *X. laevis* L4 rp-mRNA sequence (RNA-L4-UTR) using as template a plasmid containing *X. laevis* L4 cDNA, GenBank Accession Number **X052163** [18].

Annealing and melting assays

CT (sense) and [^{32}P]-5' end-labeled Comp-CT (antisense, Comp-CT*) were used for annealing assays as described elsewhere [18]. Briefly, the oligonucleotides were separately heated at 90 ºC for 3 min, and then transferred to ice for 5 min. Then, they were independently incubated in annealing buffer (50 mM Tris-HCl, pH 8.0, 0.1 mM EDTA, 1 mM DTT, 6 mM MgCl2, 80 mM KCl, and 0.1 mM ZnCl2) at 37 °C for 2 min in the absence or in the presence of the indicated recombinant protein. Finally, reaction mixtures containing CT and Comp-CT* were mixed and incubated at 37ºC. Aliquots of 20 µl were taken at specific time points as indicated and annealing reactions were stopped by adding them to 7.5 µl of stop solution (0.25% bromphenol blue, 0.25% xilene cyanol, 20% glycerol, 20 mM EDTA, 0.2% SDS, and 0.4 mg/ml yeast tRNA) and incubated at 37 °C for 1 min before being

transferred to ice. Reactions were run into 15% native PAGE in TBE 1X and gels were dried, exposed and scanned as described above. Annealing percentage was determined from the intensities of radioactive bands [18].

Melting assays were performed as described elsewhere using a pair of oligonucleotides that form a perfect duplex: CT-12 (sense: 5'- CAC CCT CCC CAC-3') and [32P]-5' end-labeled Comp-CT-12 (antisense: 5'-GTG GGG AGG GTG-3') [18]. Briefly, the pre-annealed duplex was mixed in annealing buffer with the indicated amount of protein on ice. Mixtures were sequentially incubated for 5 min at 4, 30, 40, 50 and 60 ºC in an Eppendorf Thermocycler (Mastercycler Personal). The incubation temperatures were maintained below 60 ºC since this temperature was experimentally determined as the GST-CNBP thermal denaturation value [18]. After each temperature treatment a 5-µl aliquot was taken and mixed with 5 µl of ice-cold stop solution. Reactions were run into 25% native PAGE in TBE 1X and gels were dried, exposed and scanned as described above. Melting percentage was determined from the intensities of radioactive bands [18].

Embryonic manipulation, RNA synthesis, microinjection and lineage tracing

Xenopus laevis embryos were obtained from adult organisms by standard hormone-induced egg laying and natural mating as previously described [42]. Embryos were staged according to Nieuwkoop and Faber [43]. Dejellied embryos were placed in 10% normal amphibian medium (NAM) [44] containing 5% Ficoll and the animal pole of one dorsal blastomere of four-cell stage embryos was injected with 1, 3 or 5 ng of *in vitro* transcribed capped mRNA containing 1-3 mg/ml lysine fixable fluorescein dextran (40,000 Mr; FDx, Molecular Probes) as a lineage tracer. Capped RNA was synthesized from pCS2+ vectors containing cDNA encoding $CNBP_{WT}$ or different CNBP mutants. These plasmids were linearized and transcribed with a GTP cap analog (New England Biolabs) using SP6 RNA polymerase as

previously described [42]. After DNAse treatment, RNA was phenol-chloroform extracted, ethanol- precipitated and resuspended in DEPC-treated distilled water. Approximately 8-12 nl of diluted RNA was injected into each embryo.

Embryonic protein analysis by Western blot

Embryonic proteins were obtained by treating pools of 10 dorsal halves from not injected or injected embryos at stage 15 with Sample Buffer (50mM Tris-HCl (pH 7.5); 2% (w/v) SDS; 5% (v/v) Glycerol; 0,1M DTT; and 0,1% (w/v) Bromophenol Blue) for 10 min at 60°C. Samples were centrifuged for 30 min at 21000 *g*, and proteins corresponding to one embryo were resolved in 12% SDS-PAGE. Then, proteins were transferred to Hybond-ECL nitrocellulose membranes (Amersham Biosciences – GE Helthcare) and stained for 10 min with 0.1% (w/v) PonceauS red in 1% (v/v) acetic acid. Purified recombinant $(His)_6$-CNBP was used as a positive detection control. Membranes were treated according to previous reports [5]. Anti-$(His)_6$-CNBP antibody (raised in mice) was used in a 1:1000 dilution and HRP-coupled anti-mouse antibody (Amersham Biosciences – GE Helthcare) was diluted 5000-fold. HRP activity was detected on nitrocellulose membranes by chemiluminescence using SuperSignal West Pico Chemiluminescent Substrate (Pierce). Subsequently, the membranes were used to detect actin levels using rabbit anti-actin antibody (Santa Cruz Biotechnology Inc.) in a 1:600 dilution and anti-rabbit HRP-linked antibody (Amersham Biosciences – GE Helthcare) diluted 5000-fold.

Whole-mount in situ hybridization and lineage tracing detection

Xenopus laevis embryos were fixed at stage 15 overnight in 4% (w/v) paraformaldehyde (PFA) in PBS 1X at 4ºC. After washing, embryos were stored in methanol at -20ºC until used. Antisense probes containing Digoxigenin-11-UTP were prepared for *c-myc* and *foxD3*

[37] by *in vitro* transcription. Specimens were prepared, hybridized, and stained as previously described [45] with modifications [42,46]. Detection of labeled antisense probes was performed using alkaline-phosphatase conjugated anti-digoxigenin Fab fragments (Roche Biochemicals) and with NBT/BCIP (purple) as substrate. For lineage tracer detection, the *in situ* hybridization alkaline-phosphatase reaction was stopped by incubation in methanol at 65ºC for 1 hour, then the embryos were rehydrated, blocked with 2% Roche blocking-reagent and incubated in alkaline phosphatase-conjugated anti-Fluorescein Fab fragments (Roche Biochemicals). The phosphatase activity resulting from the lineage tracing label was detected using BCIP (green) as substrate. After fixation, embryos were observed under Olympus BH-2 microscope (Olympus, Tokyo, Japan) and gene expression areas were measured by using the NIS-elements 2.3 imaging software (Nikon Instruments Inc.). Embryos displaying expression areas modified in at least 30 % in the injected side compared with the not injected side were classified as affected ones. The expression areas of the affected embryos were averaged and the observed differences were expressed as percentages of increase or decrease compared with the not injected control side.

Accession numbers

The Accession Numbers for the cDNAs and the mutant proteins produced in this work are: $CNBP_{H128A}$: GenBank **AY862150**, Entrez Protein Database **AAW62456**; $CNBP_{H128D}$: GenBank **AF232060**, Entrez Protein Database **AAF44119**; $CNBP_{H128Q}$: GenBank **AY862149**, Entrez Protein Database **AAW62455**; $CNBP_{\Delta RGG}$: GenBank **AY862153**, Entrez Protein Database **AAW62459**; $CNBP_{\Delta 1\text{-}RGG}$: GenBank **AY862151**, Entrez Protein Database **AAW62457**; $CNBP_{\Delta 5\text{-}7}$: GenBank **AY862152**, Entrez Protein Database **AAW62458**.

REFERENCES

1. Chai, Y. and Maxson, R. E., Jr. (2006). Recent advances in craniofacial morphogenesis. *Dev.Dyn.* **235,** 2353-2375.

2. Abe, Y., Chen, W., Huang, W., Nishino, M., and Li, Y. P. (2006). CNBP regulates forebrain formation at organogenesis stage in chick embryos. *Dev.Biol* **295,** 116-127.

3. Chen, W., Liang, Y., Deng, W., Shimizu, K., Ashique, A. M., Li, E., and Li, Y. P. (2003). The zinc-finger protein CNBP is required for forebrain formation in the mouse. *Development* **130,** 1367-1379.

4. Flink, I. L., Blitz, I., and Morkin, E. (1998). Characterization of cellular nucleic acid binding protein from Xenopus laevis: expression in all three germ layers during early development. *Dev.Dyn.* **211,** 123-130.

5. Weiner, A. M., Allende, M. L., Becker, T. S., and Calcaterra, N. B. (2007). CNBP mediates neural crest cell expansion by controlling cell proliferation and cell survival during rostral head development. *J Cell Biochem.* **102,** 1553-1570.

6. Rajavashisth, T. B., Taylor, A. K., Andalibi, A., Svenson, K. L., and Lusis, A. J. (1989). Identification of a zinc finger protein that binds to the sterol regulatory element. *Science* **245,** 640-643.

7. Liu, M., Kumar, K. U., Pater, M. M., and Pater, A. (1998). Identification and characterization of a JC virus pentanucleotide repeat element binding protein: cellular nucleic acid binding protein. *Virus Res.* **58,** 73-82.

8. Flink, I. L. and Morkin, E. (1995). Alternatively processed isoforms of cellular nucleic acid-binding protein interact with a suppressor region of the human beta-myosin heavy chain gene. *J.Biol.Chem.* **270,** 6959-6965.

9. Michelotti, E. F., Tomonaga, T., Krutzsch, H., and Levens, D. (1995). Cellular nucleic acid binding protein regulates the CT element of the human c-myc protooncogene. *J.Biol.Chem.* **270,** 9494-9499.

10. Konicek, B. W., Xia, X., Rajavashisth, T., and Harrington, M. A. (1998). Regulation of mouse colony-stimulating factor-1 gene promoter activity by AP1 and cellular nucleic acid-binding protein. *DNA Cell Biol.* **17,** 799-809.

11. Yasuda, J., Mashiyama, S., Makino, R., Ohyama, S., Sekiya, T., and Hayashi, K. (1995). Cloning and characterization of rat cellular nucleic acid binding protein (CNBP) cDNA. *DNA Res.* **2,** 45-49.

12. Gerbasi, V. R. and Link, A. J. (2007). The myotonic dystrophy type 2 protein ZNF9 is part of an ITAF complex that promotes cap-independent translation. *Mol.Cell Proteomics.* **6,** 1049-1058.

13. Schlatter, S. and Fussenegger, M. (2003). Novel CNBP- and La-based translation control systems for mammalian cells. *Biotechnol.Bioeng.* **81,** 1-12.

14. Ivanyi-Nagy, R., Davidovic, L., Khandjian, E. W., and Darlix, J. L. (2005). Disordered RNA chaperone proteins: from functions to disease. *Cell Mol.Life Sci.* **62,** 1409-1417.

15. Levin, J. G., Guo, J., Rouzina, I., and Musier-Forsyth, K. (2005). Nucleic acid chaperone activity of HIV-1 nucleocapsid protein: critical role in reverse transcription and molecular mechanism. *Prog.Nucleic Acid Res.Mol.Biol.* **80,** 217-286.

16. Rein, A., Henderson, L. E., and Levin, J. G. (1998). Nucleic-acid-chaperone activity of retroviral nucleocapsid proteins: significance for viral replication. *Trends Biochem.Sci.* **23,** 297-301.

17. Tompa, P. and Csermely, P. (2004). The role of structural disorder in the function of RNA and protein chaperones. *FASEB J.* **18,** 1169-1175.

18. Armas, P., Nasif, S., and Calcaterra, N. B. (2008). Cellular nucleic acid binding protein binds G-rich single-stranded nucleic acids and may function as a nucleic acid chaperone. *J.Cell Biochem.* **103,** 1013-1036.

19. McGrath, C. F., Buckman, J. S., Gagliardi, T. D., Bosche, W. J., Coren, L. V., and Gorelick, R. J. (2003). Human cellular nucleic acid-binding protein Zn2+ fingers support replication of human immunodeficiency virus type 1 when they are substituted in the nucleocapsid protein. *J.Virol.* **77,** 8524-8531.

20. Kiledjian, M. and Dreyfuss, G. (1992). Primary structure and binding activity of the hnRNP U protein: binding RNA through RGG box. *EMBO J.* **11,** 2655-2664.

21. Calcaterra, N. B., Palatnik, J. F., Bustos, D. M., Arranz, S. E., and Cabada, M. O. (1999). Identification of mRNA-binding proteins during development: characterization of Bufo arenarum cellular nucleic acid binding protein. *Dev.Growth Differ.* **41,** 183-191.

22. Armas, P., Cabada, M. O., and Calcaterra, N. B. (2001). Primary structure and developmental expression of Bufo arenarum cellular nucleic acid-binding protein: changes in subcellular localization during early embryogenesis. *Dev.Growth Differ.* **43,** 13-23.

23. Pellizzoni, L., Lotti, F., Maras, B., and Pierandrei-Amaldi, P. (1997). Cellular nucleic acid binding protein binds a conserved region of the 5' UTR of Xenopus laevis ribosomal protein mRNAs. *J.Mol.Biol.* **267,** 264-275.

24. Armas, P., Cachero, S., Lombardo, V. A., Weiner, A., Allende, M. L., and Calcaterra, N. B. (2004). Zebrafish cellular nucleic acid-binding protein: gene structure and developmental behaviour. *Gene* **337,** 151-161.

25. De Dominicis, A., Lotti, F., Pierandrei-Amaldi, P., and Cardinali, B. (2000). cDNA cloning and developmental expression of cellular nucleic acid-binding protein (CNBP) gene in Xenopus laevis. *Gene* **241,** 35-43.

26. Kingsley, P. D., Zinkin, A. S., Silver, L. S., Pendola, F. L., and Palis, J. (1996). Developmental regulation and primary structure of murine cellular nucleic acid-

binding protein, a zinc finger-containing protein whose general structure is present in evolutionarily diverse eukaryotes. *Dev.Growth Differ.* **38,** 697-706.

27. Burd, C. G. and Dreyfuss, G. (1994). Conserved structures and diversity of functions of RNA-binding proteins. *Science* **265,** 615-621.

28. Darnell, J. C., Warren, S. T., and Darnell, R. B. (2004). The fragile X mental retardation protein, FMRP, recognizes G-quartets. *Ment.Retard.Dev.Disabil.Res.Rev.* **10,** 49-52.

29. Raman, B., Guarnaccia, C., Nadassy, K., Zakhariev, S., Pintar, A., Zanuttin, F., Frigyes, D., Acatrinei, C., Vindigni, A., Pongor, G., and Pongor, S. (2001). N(omega)-arginine dimethylation modulates the interaction between a Gly/Arg-rich peptide from human nucleolin and nucleic acids. *Nucleic Acids Res.* **29,** 3377-3384.

30. Bouvet, P., Diaz, J. J., Kindbeiter, K., Madjar, J. J., and Amalric, F. (1998). Nucleolin interacts with several ribosomal proteins through its RGG domain. *J.Biol.Chem.* **273,** 19025-19029.

31. Gabus, C., Mazroui, R., Tremblay, S., Khandjian, E. W., and Darlix, J. L. (2004). The fragile X mental retardation protein has nucleic acid chaperone properties. *Nucleic Acids Res.* **32,** 2129-2137.

32. Hanakahi, L. A., Bu, Z., and Maizels, N. (2000). The C-terminal domain of nucleolin accelerates nucleic acid annealing. *Biochemistry* **39,** 15493-15499.

33. Munroe, S. H. and Dong, X. F. (1992). Heterogeneous nuclear ribonucleoprotein A1 catalyzes RNA.RNA annealing. *Proc.Natl.Acad.Sci.U.S.A* **89,** 895-899.

34. Lombardo, V. A., Armas, P., Weiner, A. M., and Calcaterra, N. B. (2007). In vitro embryonic developmental phosphorylation of the cellular nucleic acid binding protein by cAMP-dependent protein kinase, and its relevance for biochemical activities. *FEBS J.* **274,** 485-497.

35. Mayor, R. and Aybar, M. J. (2001). Induction and development of neural crest in Xenopus laevis. *Cell Tissue Res.* **305,** 203-209.

36. Steventon, B., Carmona-Fontaine, C., and Mayor, R. (2005). Genetic network during neural crest induction: from cell specification to cell survival. *Semin.Cell Dev.Biol.* **16,** 647-654.

37. Sasai, N., Mizuseki, K., and Sasai, Y. (2001). Requirement of FoxD3-class signaling for neural crest determination in Xenopus. *Development* **128,** 2525-2536.

38. Bellmeyer, A., Krase, J., Lindgren, J., and LaBonne, C. (2003). The protooncogene c-myc is an essential regulator of neural crest formation in xenopus. *Dev.Cell* **4,** 827-839.

39. Bombarda, E., Cherradi, H., Morellet, N., Roques, B. P., and Mely, Y. (2002). Zn(2+) binding properties of single-point mutants of the C-terminal zinc finger of the HIV-1 nucleocapsid protein: evidence of a critical role of cysteine 49 in Zn(2+) dissociation. *Biochemistry* **41,** 4312-4320.

40. Stote, R. H., Kellenberger, E., Muller, H., Bombarda, E., Roques, B. P., Kieffer, B., and Mely, Y. (2004). Structure of the His44 --> Ala single point mutant of the distal finger motif of HIV-1 nucleocapsid protein: a combined NMR, molecular dynamics simulation, and fluorescence study. *Biochemistry* **43,** 7687-7697.

41. Sarkar, G. and Sommer, S. S. (1990). The "megaprimer" method of site-directed mutagenesis. *Biotechniques* **8,** 404-407.

42. Aybar, M. J., Nieto, M. A., and Mayor, R. (2003). Snail precedes slug in the genetic cascade required for the specification and migration of the Xenopus neural crest. *Development* **130,** 483-494.

43. Nieuwkoop, P. D. and Faber, J. (1967) *Normal table of Xenopus laevis (Daudin); A systematical and chronological survey of the developement from the fertilized egg till the end of metamorphosis*, Second Ed., North-Holland Publishing Company, Amsterdam.

44. Slack, J. M. (1984). Regional biosynthetic markers in the early amphibian embryo. *J.Embryol.Exp.Morphol.* **80,** 289-319.

45. Harland, R. M. (1991). In situ hybridization: an improved whole-mount method for Xenopus embryos. *Methods Cell Biol.* **36,** 685-695.

46. Tribulo, C., Aybar, M. J., Nguyen, V. H., Mullins, M. C., and Mayor, R. (2003). Regulation of Msx genes by a Bmp gradient is essential for neural crest specification. *Development* **130,** 6441-6452.

FOOTNOTES

Aknowledgements: This work was supported by Grants from CONICET (PIP 6419 to NBC, and 6278 to MJA) ANPCyT-Foncyt (PICT 01-8754 to NBC, and 10623 to MJA), CIUNT-Foncyt (PICTO UNT 367 to MJA), CIUNT (to MJA). P. Armas, N. B. Calcaterra and M. J. Aybar are Staff Members while T. H. Agüero and M. Borgognone are Fellows of the Consejo Nacional de Investigaciones Científicas y Técnicas (CONICET), Argentina. We acknowledge L. I. Llarrull for helping in mutants construction, and Dr. P. Pierandrei-Amaldi for the *X. laevis* L4 ribosomal protein cDNA clone (GenBank Accession Number **X05216**).

Abbreviations: BSA, bovine serum albumin; BCIP, 5-bromo-4-chloro-3-indolyl-phosphate Toluidine salt; CNBP, cellular nucleic acid binding protein; CCHC, cysteine-cystein-histidine-cysteine; EMSA, electrophoretic mobility shift assay; FDx, fluorescein dextran; FMRP, fragile X mental retardation protein; GST, glutathione-S-transferase; HIV, human immunodeficiency virus; hnRNP, heterogeneous nuclear ribo-nuclear protein; HRP, horseradish peroxidase; NAM, normal amphibian medium; NBT, 4-nitro blue tetrazolium chloride; NC, nucleocapsid; PAGE, polyacrilamide gel electrophoresis; PCR, polymerase chain reaction; PEST, proline-glutamic acid-serine-threonine; RGG, arginine-glycine-glycine; ssDNA, single-stranded DNA; UTR, untranslated region.

FIGURE LEGENDS

Figure 1. Analysis of CNBP main structural features.

Amino acid sequence multiple alignment (CLUSTAL) of CNBP family from different vertebrate organisms (Entrez Protein Database Accession Numbers: *Bos taurus*: **AAI02299**, *Chaunus arenarum*: **AAD33937**, *Danio rerio*: **AAO73520**, *Gallus gallus*: **AAB62243**, *Homo sapiens*: **AAA61975**, *Mus musculus*: **AAB60490**, *Rattus norvegicus*: **BAA08212**, *Xenopus laevis*: **CAA69031**, *Xenopus tropicalis*: **AAI22021**). The seven CCHC zinc knuckle motifs are boxed in gray, the RGG box motif is boxed in black, and the putative PEST proteolytic site is signaled by an arrow.

Figure 2. CNBP amino acid and deletion site-directed mutants.

Schematic representation of the wild type *Chaunus arenarum* CNBP ($CNBP_{WT}$), amino acid ($CNBP_{H128A}$, $CNBP_{H128D}$, $CNBP_{H128Q}$), and deletion ($CNBP_{\Delta RGG}$, $CNBP_{\Delta 1\text{-}RGG}$, $CNBP_{\Delta 5\text{-}7}$) site-directed mutants motif patterns. Numbers below each scheme indicate the amino acid position in the $CNBP_{WT}$ amino acid sequence.

Figure 3. CNBP amino acid site-directed mutants binding to single-stranded nucleic acids.

EMSAs performed using GST-$CNBP_{WT}$, GST-$CNBP_{H128A}$, GST-$CNBP_{H128Q}$, and GST-$CNBP_{H128D}$. GST was used as a control. Free and shifted probes are indicated by arrows at the left of the figure. (a) EMSAs performed using the labeled RNA-L4-UTR probe. (b)

EMSAs performed with the labeled Comp-CT probe. (c) EMSAs performed using the labeled DNA-L4-UTR probe.

Figure 4. CNBP deletion site-directed mutants binding to single-stranded nucleic acids.

EMSAs performed using GST-CNBP$_{WT}$, GST-CNBP$_{\Delta 5\text{-}7}$, GST-CNBP$_{\Delta 1\text{-}RGG}$ and GST-CNBP$_{\Delta RGG}$. GST was used as a control. Free and shifted probes bands are indicated by arrows at the left of the figure. (a) EMSAs performed using the labeled RNA-L4-UTR probe. (b) EMSAs performed with the labeled Comp-CT probe. (c) EMSAs performed using the labeled DNA-L4-UTR probe.

Figure 5. Nucleic acid annealing promotion activity of CNBP mutants.

Annealing assay using labeled Comp-CT and unlabeled CT oligonucleotides. Controls without protein or with GST were included. Lanes corresponding to the labeled Comp-CT probe alone and the completely annealed reaction (annealed CT+Comp-CT) are also shown. In all cases final protein concentration was 0.1 μM, which represented a molar protein:probe ratio of 10:1. Reactions were sampled at 0, 1, 3, 10, and 30 minutes. Single-stranded (ss) and double-stranded (ds) probes are indicated at the right of each figure. (a) Annealing assay performed with GST-CNBP$_{WT}$, GST-CNBP$_{\Delta 5\text{-}7}$, GST-CNBP$_{H128A}$, GST-CNBP$_{H128Q}$, and GST-CNBP$_{H128D}$. (b) Annealing assay performed with GST-CNBP$_{WT}$, GST-CNBP$_{\Delta 1\text{-}RGG}$, and GST-CNBP$_{\Delta RGG}$. (c) Bar chart representing annealing percentage (%) obtained at 30 minutes (means ± SEM, n = 3). Statistically significant differences are indicated, ** indicates $p < 0.01$ and * indicates $p < 0.05$ in respect of the controls (one way ANOVA, Tuckey test).

Figure 6. Nucleic acid melting promotion activity of CNBP deletion mutants.

(a) Melting assays using a pre-annealed duplex formed by labeled Comp-CT-12 and unlabeled CT-12 oligonucleotides. Melting assays were performed with GST-$CNBP_{WT}$, GST-$CNBP_{\Delta 5\text{-}7}$, GST-$CNBP_{\Delta 1\text{-}RGG}$, and GST-$CNBP_{\Delta RGG}$. Control reactions were carried out without protein or by adding 10 μM GST. In all cases final protein concentration was 10 μM, which represented a molar protein:probe ratio of 1000:1. Reactions were sampled at 4, 30, 40, 50, and 60ºC. The calculated melting temperatures (T_m) are indicated for each experimental condition. Single-stranded (ss) and double-stranded (ds) probes are indicated at the right of the gels. (b) EMSAs performed with the labeled Comp-CT probe and GST-$CNBP_{WT}$, GST-$CNBP_{\Delta 5\text{-}7}$, GST-$CNBP_{\Delta 1\text{-}RGG}$ and GST-$CNBP_{\Delta RGG}$. Proteins were maintained at 4°C (left) or thermally stressed by sequential incubation for 5 min at 30, 40, 50, and 60ºC (right). A similar reduction in affinity (increment in K_d) of 2- to 3-fold was observed for GST-$CNBP_{WT}$ as well as for deletion mutants.

Figure 7. *In vivo* effects of CNBP overexpression on the neural crest specification of *Xenopus* embryos.

One dorsal blastomere of 4-cell stage *Xenopus laevis* embryos was injected with *in vitro* transcribed capped mRNA (3 ng/embryo) and FDx as lineage tracer. Embryos at stage 15 are shown in a dorsal view. The injected side (indicated by an arrow head) was recognized by the detection of the lineage tracer FDx (turquoise). (a, b) Expression territory of neural crest markers *foxd3* and *c-myc* was expanded on the $CNBP_{WT}$ mRNA-injected side. (c-f) The expression territory of *foxd3* and *c-myc* markers in the prospective neural crest domain was

reduced in the injected side of embryos injected with $CNBP_{\Delta RGG}$ (c, d) and $CNBP_{\Delta 1\text{-}RGG}$ (e, f) mRNAs. The co-injection of $CNBP_{\Delta RGG}$ (g, h) or $CNBP_{\Delta 1\text{-}RGG}$ (i, j) mRNAs and $CNBP_{WT}$ mRNA rescued the *foxd3* and *c-myc* expression territory patterns in the injected side.